Dynamics of flight of the fragments with higher order Haar wavelet method

Lenart Kivistik*, Marmar Mehrparvar, Martin Eerme and Jüri Majak

Department of Mechanical and Industrial Engineering, Tallinn University of Technology, Ehitajate tee 5, 19086 Tallinn, Estonia

Abstract. Fragments that have an irregular shape and move at high speeds are difficult to assess since experiments require high-tech solutions, and the differential equations that describe the motion cannot be solved analytically. Different numerical and function approximation methods are used to find the trajectory model. This work uses a state-of-the-art, higher order Haar wavelet method to approximate the trajectory model with empirically determined drag force. The initial conditions of the flight of the fragments are determined by the finite element method. The results obtained by utilizing the Haar wavelet method and the higher order Haar wavelet method are compared. The higher order Haar wavelet method outperforms the Haar wavelet method but allows for keeping the implementation complexity of the method in the same range. Utilizing the higher order Haar wavelet method leads to a reduction in the computational cost since the same accuracy with the Haar wavelet method can be achieved with the use of several order lower mesh.

1. INTRODUCTION

The study of the flight of fragments provides an opportunity to assess the risk of fast-moving fragments thrown into the environment. The risk of fragments depends on the density of fragments per volume unit and the kinetic energy of the investigated fragment at the location under consideration [1]. The initial parameters of fragmentation are determined by the fragmenting object and the nature of the formation. The fragmenting objects can be fuel tanks, explosive devices, vehicle body parts, etc., and the nature of the formation is mostly explosion, collision, or fracture. Simulations, experiments, and statistical models are used to study the fragments produced by the explosion. Conducting experiments and collecting the information necessary for the flight of fragments, such as fragment mass, dimensions, velocities, accelerations, and direction vectors, are resource- and labor-intensive [2–4]. Statistical models can be used in limited situations based on specific experiments and may not be appropriate for a specific case [5]. Djelosevic and Tepic introduced the probabilistic mass method [6], Ahmed et al. utilized the arbitrary Lagrangian–Eulerian approach [3], and Ugrčić adapted the stochastic failure theory [7] fragmentation analysis of metallic objects. The simulation results can be utilized as initial data for the point mass trajectory model, described by a nonlinear system of ordinary differential equations (ODE). Kljuno and Catovic [8], Szmelter and Lee [9] used the Runge–Kutta

---
* Corresponding author, lenart.kivistik@taltech.ee

numerical method, and Djelosevic and Tepic [6] used the Taylor series numerical method to solve the ODE system.

For the purpose of solving the trajectory system of equations, herein two recent numerical methods, the Haar wavelet method (HWM) and the higher order Haar wavelet method (HOHWM), are implemented. The HWM, introduced in 1997 by Chen and Hsiao, has been applied with success for solving a wide class of differential and integro-differential equations [10–14]. Pioneering work in the development and application of the HWM was done by Lepik, who considered integer and fractional differential equations as well as integro-differential equations, covering a wide class of problems from mathematics, physics, and evolution equations [10,15–20]. The HWM is known as a method with simple implementation since it is based on the simplest wavelet [10]. Recently, the HWM was applied with success for solving Bratu-type equations [21] – singularly perturbed differential equations with integral boundary conditions [22]. In [23–26], the HWM is combined with AI methods and tools. However, the rate of convergence of the HWM is two, i.e., rather humble. In 2018, the HOHWM was introduced as the principal improvement of the HWM [27]. The rate of convergence of the HOHWM depends on the method parameter and, in simpler cases, is equal to four. The HOHWM has been utilized with success by a number of authors in [28–39] for solving a wide class of ODE [28–33], partial differential equations [34], and fractional Fredholm integro-differential equations [35], but needs still further validation with more complex problems. Herein, the HWM and HOHWM are adapted for solving nonlinear systems of trajectory equations of the fragments.

2. FORMULATION

In this section, the formulation of the flight dynamics of fragments is developed. Beforehand, initial coordinate values, velocity values with regard to coordinates, air density, fragment mass, drag coefficient, and exposed area are all necessary. Next, the trajectory model is simplified, which is then solved by employing the higher order Haar wavelet method.

2.1. Flight dynamics of the fragments

The natural fragmentation simulation of an explosive projectile shell is based on the finite element method and stochastic failure theory and is simulated in the ANSYS AUTODYN software.

The arbitrary Lagrangian–Eulerian approach with the Johnson–Cook strength and fracture method is used to simulate fragmentation and the propagation of fragments into the surrounding air. Numerical analyses determine the fragment's initial position, velocity, mass, and volume. The coordinate system of the simulation is based on the CAD model and is transformed into the coordinate system of the situation. On the rear surface of the unfragmented projectile, the z-axis intersects with the axis of symmetry of the projectile and is at an angle of 60 degrees from the ground. The xy-plane represents the ground surface. Figure 1 visualizes the geometry used in the simulation, the coordinate system, and the scattering of fragments caused by the explosion.

2.2. Trajectory model of the fragments

The path of a fragment moving while being affected by drag and gravitational force can be predicted using the point mass trajectory model based on the Lord Rayleigh's drag equation [5,9,40]:

$$
\begin{aligned}
x'' &= -\frac{A\rho C_D}{2m}\sqrt{x'^2 + y'^2 + z'^2} \cdot x', \\
y'' &= -\frac{A\rho C_D}{2m}\sqrt{x'^2 + y'^2 + z'^2} \cdot y', \\
z'' &= -\frac{A\rho C_D}{2m}\sqrt{x'^2 + y'^2 + z'^2} \cdot z' - g,
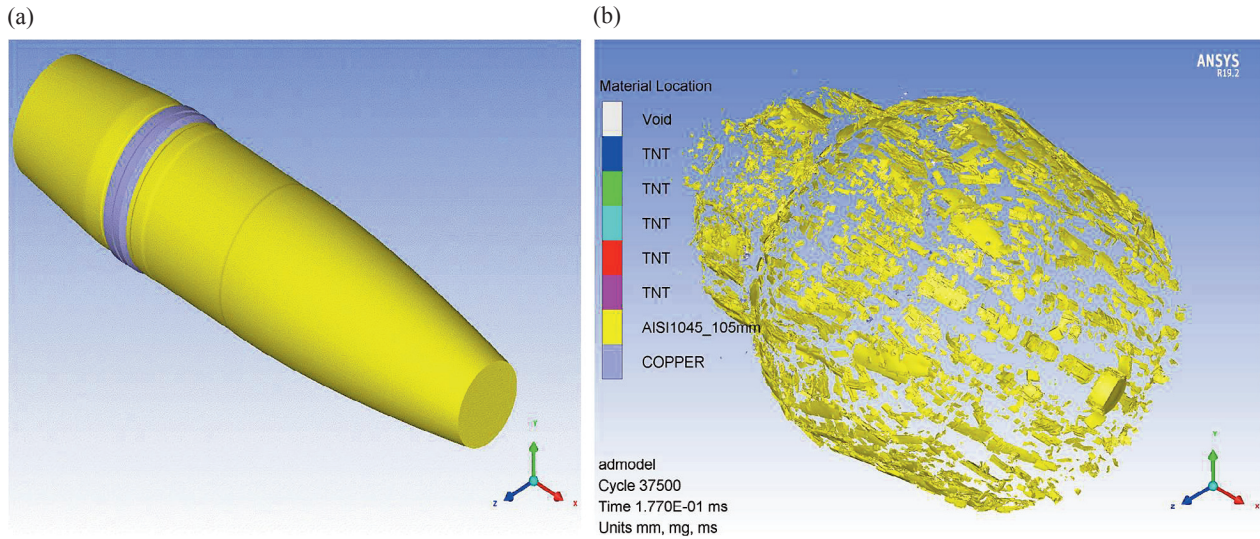\end{aligned}
\tag{1}
$$

(a)

(b)

Fig. 1. Unfragmented projectile (a) and fragmentation and propagation of fragments (b).

where x', y' and z' are velocities in each direction, $\rho = 1.20 \frac{kg}{m^3}$ is the air density, and $g = 9.81 \; m/s^2$ is the gravitational acceleration. Also, C_D is the drag coefficient, which as a rule is affected by the Mach number. Still, $C_D = 0.6$ is the result of the most common simplification applied in this study, which assumes a constant drag coefficient [5]. A few mathematical operations are carried out in order to build a solution for the system of differential equations; in Eq. (1) the value of y can be found in terms of x:

$$\frac{x''}{x'} = \frac{y''}{y'} \quad \rightarrow \quad y = cx + d \; , \; c = \frac{y_0'}{x_0'} \; , d = y_0 - \frac{y_0'}{x_0'} \cdot x_0. \tag{2}$$

Quasilinearization is a numerical method that solves a series of linearized problems iteratively in order to estimate the solution of the nonlinear differential system of equations. Essentially, quasilinearization involves linearizing the nonlinear problem around the current estimate of the solution at each iteration, solving the resulting linearized problem and using the solution to update the estimate of the solution to the original nonlinear problem. Until convergence is reached, this process is continued iteratively. Then, by substituting $\frac{A\rho C_D}{2m} = k$, the system of three equations can be reduced to two equations:

$$
\begin{aligned}
x'' &= -k\sqrt{(1 + c^2)x'^2 + z'^2} \; x' = f_1(x', z'), \\
z'' &= -k\sqrt{(1 + c^2)x'^2 + z'^2} \; z' - g = f_2(x', z').
\end{aligned}
\tag{3}
$$

In order to linearize the nonlinear systems, the Taylor series expansion has been utilized in Eq. (4):

$$
\begin{aligned}
x''_{n+1} &= f_1(x'_n, z'_n) + (x'_{n+1} - x'_n)\frac{\partial f_1}{\partial x'_n} + (z'_{n+1} - z'_n)\frac{\partial f_1}{\partial z'_n}, \\
z''_{n+1} &= f_2(x'_n, z'_n) + (z'_{n+1} - z'_n)\frac{\partial f_2}{\partial z'_n} + (x'_{n+1} - x'_n)\frac{\partial f_2}{\partial x'_n},
\end{aligned}
\tag{4}
$$

where

$$\frac{\partial f_1}{\partial x'} = -k \left[\frac{(1 + c^2)x' \cdot x'}{\sqrt{(1 + c^2)x'^2 + z'^2}} + \sqrt{(1 + c^2)x'^2 + z'^2} \right],$$

$$\frac{\partial f_1}{\partial z'} = -k \left[\frac{x' \cdot z'}{\sqrt{(1 + c^2)x'^2 + z'^2}} \right],$$

$$\frac{\partial f_2}{\partial x'} = -k \left[\frac{(1 + c^2)x' \cdot z'}{\sqrt{(1 + c^2)x'^2 + z'^2}} \right], \tag{5}$$

$$\frac{\partial f_2}{\partial z'} = -k \left[\frac{z' \cdot z'}{\sqrt{(1 + c^2)x'^2 + z'^2}} + \sqrt{(1 + c^2)x'^2 + z'^2} \right].$$

2.3. Higher order Haar wavelet method

The discontinuous Haar wavelet, a specific family of discrete orthonormal wavelets with a step function-like appearance, is one of the most basic wavelets. A basis, whose components are orthonormal to each other and normalized to the unit length, is made up of the additional wavelets that are derived from the same basic wavelet. This property allows wavelet coefficients to be computed independently of each other. The functions for Haar are given as:

$$h_i(x) = \begin{cases} 1 & \text{for} & x \in [\alpha(i), \beta(i)) \\ -1 & \text{for} & x \in [\beta(i), \gamma(i)) \\ 0 & \text{elsewhere,} \end{cases} \tag{6}$$

where

$$\begin{aligned}
\alpha(i) &= A + 2k\mu\Delta x, \\
\beta(i) &= A + (2k + 1)\mu\Delta x, \\
\gamma(i) &= A + 2(k + 1)\mu\Delta x, \\
i &= m + k + 1, \ \mu = \frac{M}{m}, \ \Delta x = \frac{B-A}{2M},
\end{aligned} \tag{7}$$

where integer $k = 0, 1, \ldots, m - 1$ specifies the location of the particular square wave, and $m = 2^j$ is the maximum number of square waves arranged in the interval $[A, B]$. Hence, the integrals of the Haar functions of order n can be presented as in [14]:

$$p_{n,i}(x) = \begin{cases} 0 & x \in [A, \alpha(i)) \\ \dfrac{(x - \alpha(i))^n}{n!} & x \in [\alpha(i), \beta(i)) \\ \dfrac{(x - \alpha(i))^n - 2(x - \beta(i))^n}{n!} & \text{for} \quad x \in [\beta(i), \gamma(i)) \\ \dfrac{(x - \alpha(i))^n - 2(x - \beta(i))^n + (x - \gamma(i))^n}{n!} & x \in [\gamma(i), B) \\ 0 & \text{elsewhere.} \end{cases} \tag{8}$$

As mentioned before, the higher order Haar wavelet techniques make it easier to analyze complicated data patterns more precisely, capturing minute details and subtle fluctuations. This improved resolution is especially helpful in situations where a greater degree of information is essential for correctly interpreting and comprehending the underlying dynamics. The higher order wavelet expansion is introduced in [27]:

$$\frac{d^{n+2s} f(x)}{dx^{n+2s}} = \sum_{i=1}^{\infty} a_i h_i(x), \ s = 1, 2, \ldots. \tag{9}$$

In Eq. (9), a_i is a component of the unknown coefficient vector. Finally, the method's numerical order of convergence can then be calculated based on [14]:

$$\text{Convergence rate} = \log\left(\frac{F_{i-1}-F_e}{F_i-F_e}\right)/\log(2), \tag{10}$$

where F_e is the existing solution in the literature.

3. NUMERICAL RESULTS

A projectile with a mass of 12 kg and a diameter of 105 mm was used in the simulation as a case study. The 0.17 ms simulation produced about 3950 fragments. Of these fragments, one was selected based on its initial location and velocity. The fragment's location and velocity with respect to the x-axis were then determined using the formulation given in the previous section, and were compared to the results from the HWM (Table 1). The convergence rate in both cases was calculated by Eq. (10), in which F_e was obtained by utilizing the well-known Runge–Kutta method as a reference at $t = 2.5$ s.

In Table 1, N is the number of collocation points, $N = 2 \cdot m$. As can be observed, in the case of the HOHWM, the absolute error decreases and converges much faster compared to the HWM, allowing for fewer collection points to achieve an accurate result. In Table 2, the results of the location and velocities in each direction are gathered for the same fragment mentioned before at various time steps.

It should be mentioned that since the initial values of coordinates and velocities are in a wide range, an accurate method, such as the utilized HOHWM, and a precise programming process are needed to achieve an accurate result.

Table 1. Comparison of HWM and HOHWM for selected fragment at $t = 2.5$ s

s	N	x	Error	Convergence rate	x'	Error	Convergence rate
HWM ($s = 0$)	4	–17.29994925	1.28E–01		–2.78958350	9.85E–02	
	8	–17.39615158	3.18E–02	2.0103933	–2.86413772	2.40E–02	2.0383492
	16	–17.42001639	7.93E–03	2.0030078	–2.88213661	5.99E–03	2.0015815
	32	–17.42596710	1.98E–03	2.0007748	–2.88663071	1.50E–03	2.0009089
	64	–17.42745378	4.95E–04	2.0001951	–2.88775339	3.74E–04	2.0003872
	128	–17.42782539	1.24E–04	2.0000489	–2.88803396	9.35E–05	2.0000500
	256	–17.42791828	3.10E–05	2.0000122	–2.88810410	2.34E–05	2.0000246
HOHWM ($s = 1$)	4	–17.42072359	7.23E–03		–2.88349768	4.63E–03	
	8	–17.42751557	4.34E–04	4.0576692	–2.88784956	2.78E–04	4.0581877
	16	–17.42792242	2.68E–05	4.0146075	–2.88811028	1.72E–05	4.0142098
	32	–17.42794758	1.67E–06	4.0036622	–2.88812641	1.07E–06	4.0046429
	64	–17.42794915	1.04E–07	4.0009162	–2.88812741	6.69E–08	4.0008970
	128	–17.42794924	6.53E–09	4.0002289	–2.88812748	4.18E–09	4.0002293
	256	–17.42794925	4.08E–10	4.0000549	–2.88812748	2.61E–10	4.0000268

Runge–Kutta method: –17.42794925   Runge–Kutta method: –2.88812748

Table 2. Position and velocities of selected fragment at various time steps

t	x	y	z	x'	y'	z'
initial	0.1143	−0.1703	0.8062	−24.2968	−1121.0214	69.5044
0.5 s	−7.3394	−344.8664	21.2146	−9.8396	−455.8405	24.7261
1 s	−11.2112	−524.3401	29.8954	−6.14743	−285.0912	11.4625
1.5 s	−13.8546	−646.9589	33.7039	−4.4587	−206.8792	4.0389
2 s	−15.8341	−738.8114	34.3712	−3.5065	−162.7054	−1.2054
2.5 s	−17.4279	−812.8022	32.6808	−2.8881	−134.0709	−5.4658

4. CONCLUSION

Using finite element analysis, the mass and shape of the fragments, their initial positions, and velocities have been determined. The numerical solution of the fragment trajectory model was performed using the higher order Haar wavelet method with a simplified approach for modeling drag coefficient behavior. The HWM solution has been developed as a reference solution. The rates of convergence obtained by applying HWM and HOHWM were equal to two and four, respectively. The HOHWM provides possibilities for further increase of accuracy (by changing method parameters), but in the latter case, a remarkable increase of the implementation complexity can be observed. Higher accuracy with the same mesh used or equal accuracy with a lower mesh achieved by HOHWM leads to saving computing time, i.e., energy resources, etc.

ACKNOWLEDGMENTS

REFERENCES

1. Kokinakis, W. and Sperrazza, J. Criteria for incapacitating soldiers with fragments and flechettes. *Ballist. Res. Lab.*, 1965.
2. Angel, J. *Methodology for Dynamic Characterization of Fragmenting Warheads*. Army Research Laboratory, Aberdeen, 2009.
3. Ahmed, K., Malik, A. Q., Hussain, A., Ahmad, I. R. and Ahmad, I. Blast and fragmentation studies of a scaled down artillery shell-simulation and experimental approaches. *Int. J. Multiphys.*, 2021, **15**(1), 49–71. https://doi.org/10.21152/1750-9548.15.1.49
4. Arnold, W. and Rottenkolber, E. Fragment mass distribution of metal cased explosive charges. *Int. J. Impact Eng.*, 2008, **35**(12), 1393–1398. https://doi.org/10.1016/j.ijimpeng.2008.07.049
5. Zecevic, B., Terzic, J., Catovic, A. and Serdarevic-Kadic, S. Characterization of distribution parameters of fragment mass and number for conventional projectiles. In *Proceedings of the New Trends in Research of Energetic Materials, Czech Republic, 13 April 2011*. 1026–1039.
6. Djelosevic, M. and Tepic, G. Probabilistic simulation model of fragmentation risk. *J. Loss Prev. Process Ind.*, 2019, **60**, 53–75. https://doi.org/10.1016/j.jlp.2019.04.003

7. Ugrčić, M. and Ivanišević, M. Characterization of the natural fragmentation of explosive ordnance using the numerical techniques based on the FEM. *Sci. Tech. Rev.*, 2015, **65**(4), 16–27. https://doi.org/10.5937/str1504016u

8. Kljuno, E. and Catovic, A. Trajectory estimation model for a solid body with an irregular shape undergoing extremely high aerodynamic forces. *Period. Eng. Nat. Sci.*, 2021, **9**(2). https://doi.org/10.21533/pen.v9i2.1694

9. Szmelter, J. and Kiat Lee, C. Prediction of fragment distribution and trajectories of exploding shells. *J. Battlef. Technol.*, 2007, **10**(3), 1–6.

10. Lepik, Ü. and Hein, H. Applying Haar wavelets in the optimal control theory. In *Haar Wavelets. Mathematical Engineering*. Springer, Cham, 2014, 123–135. https://doi.org/10.1007/978-3-319-04295-4_9

11. Pervaiz, N. and Aziz, I. Haar wavelet approximation for the solution of cubic nonlinear Schrodinger equations. *Phys. A: Stat. Mech. Appl.*, 2020, **545**, 123738. https://doi.org/10.1016/j.physa.2019.123738

12. Aziz, I. and Khan, I. Numerical solution of diffusion and reaction-diffusion partial integro-differential equations. *Int. J. Comput. Methods*, 2018, **15**(6). https://doi.org/10.1142/S0219876218500470

13. Siraj-ul-Islam, Aziz, I. and Al-Fhaid, A. S. An improved method based on Haar wavelets for numerical solution of nonlinear integral and integro-differential equations of first and higher orders. *J. Comput. Appl. Math.*, 2014, **260**, 449–469. https://doi.org/10.1016/j.cam.2013.10.024

14. Majak, J., Shvartsman, B., Karjust, K., Mikola, M., Haavajõe, A. and Pohlak, M. On the accuracy of the Haar wavelet discretization method. *Compos. B Eng.*, 2015, **80**, 321–327. https://doi.org/10.1016/j.compositesb.2015.06.008

15. Lepik, Ü. Solving PDEs with the aid of two-dimensional Haar wavelets. *Comput. Math. with Appl.*, 2011, **61**(7), 1873–1879. https://doi.org/10.1016/j.camwa.2011.02.016

16. Lepik, Ü. Numerical solution of differential equations using Haar wavelets. *Math. Comput. Simul.*, 2005, **68**(2), 127–143. https://doi.org/10.1016/j.matcom.2004.10.005

17. Lepik, Ü. Haar wavelet method for nonlinear integro-differential equations. *Appl. Math. Comput.*, 2006, **176**(1), 324–333. https://doi.org/10.1016/j.amc.2005.09.021

18. Lepik, Ü. Application of the Haar wavelet transform to solving integral and differential equations. *Proc. Estonian Acad. Sci.*, 2007, **56**(1), 28–46. https://doi.org/10.3176/phys.math.2007.1.03

19. Lepik, Ü. Numerical solution of evolution equations by the Haar wavelet method. *Appl. Math. Comput.*, 2007, **185**(1), 695–704. https://doi.org/10.1016/j.amc.2006.07.077

20. Lepik, Ü. Solving fractional integral equations by the Haar wavelet method. *Appl. Math. Comput.*, 2009, **214**(2), 468–478. https://doi.org/10.1016/j.amc.2009.04.015

21. Swati, Singh, M. and Singh, K. An advancement approach of Haar wavelet method and Bratu-type equations. *Appl. Numer. Math.*, 2021, **170**, 74–82. https://doi.org/10.1016/j.apnum.2021.07.014

22. Ahsan, M., Bohner, M., Ullah, A., Khan, A. A. and Ahmad, S. A Haar wavelet multi-resolution collocation method for singularly perturbed differential equations with integral boundary conditions. *Math. Comput. Simul.*, 2023, **204**, 166–180. https://doi.org/10.1016/j.matcom.2022.08.004

23. Hein, H. and Jaanuska, L. Quantification of cracks in beams on the Pasternak foundation using Haar wavelets and machine learning. *Proc. Estonian Acad. Sci.*, 2022, **71**(1), 16–29. https://doi.org/10.3176/proc.2022.1.02

24. Jaanuska, L. and Hein, H. Delamination quantification by Haar wavelets and machine learning. *Mech. Compos. Mater.*, 2022, **58**, 249–260. https://doi.org/10.1007/s11029-022-10025-2

25. Hein, H. and Jaanuska, L. Comparison of machine learning methods for crack localization. *Acta Comment. Univ. Tartu. Math.*, 2019, **23**(1). https://doi.org/10.12697/ACUTM.2019.23.13

26. Hein, H. and Jaanuska, L. Detection and classification of cracking in nonlocal nanobeams using modal data and Haar wavelets. *AIP Conf. Proc.*, 2023, **2849**(1), 250004. https://doi.org/10.1063/5.0162292

27. Majak, J., Pohlak, M., Karjust, K., Eerme, M., Kurnitski, J. and Shvartsman, B. S. New higher order Haar wavelet method: application to FGM structures. *Compos. Struct.*, 2018, **201**, 72–78. https://doi.org/10.1016/j.compstruct.2018.06.013

28. Arda, M., Majak, J. and Mehrparvar, M. Longitudinal wave propagation in axially graded Raylegh–Bishop nanorods. *Mech. Compos. Mater.*, 2024, **59**, 1109–1128. https://doi.org/10.1007/s11029-023-10160-4

29. Sorrenti, M., Di Sciuva, M., Majak, J. and Auriemma, F. Static response and buckling loads of multilayered composite beams using the refined zigzag theory and higher-order Haar wavelet method. *Mech. Compos. Mater.*, 2021, **57**, 1–18. https://doi.org/10.1007/s11029-021-09929-2

30. Majak, J., Shvartsman, B., Ratas, M., Bassir, D., Pohlak, M., Karjust, K. et al. Higher-order Haar wavelet method for vibration analysis of nanobeams. *Mater. Today Commun.*, 2020, **25**, 101290. https://doi.org/10.1016/j.mtcomm.2020.101290

31. Mehrparvar, M., Majak, J., Karjust, K. and Arda, M. Free vibration analysis of tapered Timoshenko beam with higher order Haar wavelet method. *Proc. Estonian Acad. Sci.*, 2022, **71**(1), 77–83. https://doi.org/10.3176/proc.2022.1.07

32. Mehrparvar, M., Majak, J. and Karjust, K. Free vibration analysis of Timoshenko beam by higher-order Haar wavelet method. *AIP Conf. Proc.*, 2023, **2849**(1), 250007. https://doi.org/10.1063/5.0162269

33. Arda, M., Karjust, K. and Mehrparvar, M. Wave propagation in axially graded carbon nanotubes. *AIP Conf. Proc.*, 2023, **2849**(1), 250006. https://doi.org/10.1063/5.0162668

34. Ratas, M., Salupere, A. and Majak, J. Solving nonlinear PDEs using the higher order Haar wavelet method on nonuniform and adaptive grids. *Math. Model. Anal.*, 2021, **26**(1). https://doi.org/10.3846/mma.2021.12920

35. Darweesh, A., Al-Khaled, K. and Al-Yaqeen, O. A. Haar wavelets method for solving class of coupled systems of linear fractional Fredholm integro-differential equations. *Heliyon*, 2023, **9**(9), e19717. https://doi.org/10.1016/j.heliyon.2023.e19717

36. Ahsan, M., Lei, W., Khan, A. A., Ahmed, M., Alwuthaynani, M. and Amjad, A. A higher-order collocation technique based on Haar wavelets for fourth-order nonlinear differential equations having nonlocal integral boundary conditions. *Alex. Eng. J.*, 2024, **86**, 230–242. https://doi.org/10.1016/j.aej.2023.11.066

37. Swati, Singh, M. and Singh, K. An efficient technique based on higher order Haar wavelet method for Lane–Emden equations. *Math. Comput. Simul.*, 2023, **206**, 21–39. https://doi.org/10.1016/j.matcom.2022.10.031

38. Bulut, F., Oruç, Ö. and Esen, A. Higher order Haar wavelet method integrated with strang splitting for solving regularized long wave equation. *Math. Comput. Simul.*, 2022, **197**, 277–290. https://doi.org/10.1016/j.matcom.2022.02.006

39. Ahsan, M., Lei, W., Khan, A. A., Ullah, A., Ahmad, S., Arifeen, S. U. et al. A high-order reliable and efficient Haar wavelet collocation method for nonlinear problems with two point-integral boundary conditions. *Alex. Eng. J.*, 2023, **71**, 185–200. https://doi.org/10.1016/j.aej.2023.03.011

40. Moxnes, J. F., Frøyland, Ø., Øye, I. J., Brate, T. I., Friis, E., Ødegårdstuen, G. et al. Projected area and drag coefficient of high velocity irregular fragments that rotate or tumble. *Def. Technol.*, 2017, **13**(4), 269–280. https://doi.org/10.1016/j.dt.2017.03.008

Fragmendi lennudünaamika analüüs kõrgemat järku Haari lainikute meetodi abil

Lenart Kivistik, Marmar Mehrparvar, Martin Eerme ja Jüri Majak

Ebakorrapärase kujuga ja suurel kiirusel liikuvate fragmentide lennudünaamika on komplitseeritud, mistõttu seda on raske hinnata, kuna katsed eeldavad kõrgtehnoloogilisi lahendusi ning liikumist kirjeldavad diferentsiaalvõrrandid pole analüütiliselt lahendatavad. Trajektoori mudeli koostamiseks leiab kirjandusest erinevaid numbrilisi algoritme. Artiklis on kasutatud empiiriliselt määratud õhutakistusega trajektoori mudeli lähendamiseks kõrgemat järku Haari lainikute meetodit. Fragmentide lennu algtingimused on määratud lõplike elementide meetodi abil. Võrreldud on Haari lainikute ja kõrgemat järku Haari lainikute meetodite tulemusi. Selgub, et sama keerukuse korral tagab kõrgemat järku Haari lainikute meetod suurema täpsuse kui Haari lainikute meetod. Kõrgemat järku Haari lainikute meetodi kasutamine võimaldab vähendada arvutusmahtu, kuna võrdlusmeetodiga sama täpsus saavutati mitu järku madalamat arvutusvõrku kasutades.